FOREX Publication
Open Access | Rapid and quality publishing

International Journal of Electrical and Electronics Research (IJEER)
Research Article | Volume 12, Issue 4 | Pages 1418-1426 | e-ISSN: 2347-470X

Linearization, EM Simulation, and Realization of a 40 DBM Class-AB Gan Power Amplifier

Said Elkhaldi[1*], Moustapha El Bakkali[2], Naima Amar Touhami[3], Taj-eddin Elhamadi[4], and Hmamou Abdelmounim[5]

[1]*Experimentation and Modeling in Mechanics and Energy Systems, National School of Applied Sciences Abdelmalek Essaadi University, Al Hoceima, Morocco; s.elkhaldi@uae.ac.ma*
[2,3,4] *Intelligent Systems Design (ISD) laboratory, Electronic and smart systems (ESS) team, Faculty of Sciences, Abdelmalek Essaadi University, Tétouan, Morocco*
[5]*Faculty of science and technology, Moulay Ismail University of Meknes, Morocco*

***Correspondence:** Said Elkhaldi; *s.elkhaldi@uae.ac.ma*

ABSTRACT- This research article presents the comprehensive design and analysis of a 2.45 GHz RF power amplifier operating at 40 dBm using GaN technology. The amplifier is built around the CGH40010F transistor and employs a Linearization with Nonlinear Components Method (LINC) for enhanced linearity. The study outlines the design methodology, including the selection of the CGH40010F transistor and the application of the LINC technique. It investigates the amplifier's performance characteristics, including power output, linearity, and efficiency at the 2.45 GHz frequency. The findings reveal a robust Class-AB GaN power amplifier capable of delivering 40 dBm of power while maintaining excellent linearity, making it suitable for demanding RF applications. The utilization of GaN technology and the LINC method demonstrates the potential for achieving high-performance amplifiers in modern wireless communication systems. In conclusion, this article provides valuable insights into the design and linearization of high-power GaN amplifiers, showcasing the capabilities of the CGH40010F transistor and the effectiveness of the LINC technique for achieving superior performance in RF power amplification.

Keywords: GaN transistor, Power amplifier, Gain, PAE, Linearization, LINC.

ARTICLE INFORMATION

Author(s): Said Elkhaldi, Moustapha El Bakkali, Naima Amar Touhami, Taj-eddin Elhamadi, Hmamou Abdelmounim;

Received: 20/07/2024; **Accepted**: 11/09/2024; **Published**: 30/12/2024;
e-ISSN: 2347-470X;
Paper Id: IJEER 2007-20;
Citation: 10.37391/IJEER.120436
Webpage-link:
https://ijeer.forexjournal.co.in/archive/volume-12/ijeer-120436.html

1. INTRODUCTION

Power amplifiers (PAs) are essential components of wireless communication systems, responsible for amplifying signals before transmission. However, as the demand for higher data rates and more efficient wireless communication systems increases the linearity of PAs becomes a critical factor in their performance. The LINC (Linear Amplification with Nonlinear Components) method is a well-known technique for linearizing PAs while maintaining high efficiency [1]. This method is particularly effective in GaN-based PAs, which are commonly used in high-power applications such as cellular base stations and satellite communication systems [2].

Recent research has focused on improving the performance of LINC-based GaN PAs, through various approaches such as modified LINC architectures, digital pre-distortion (DPD) techniques, and machine learning-based methods. For instance, a novel LINC architecture with a hybrid active/passive predistorter was proposed to achieve higher linearity and reduce the complexity of the system [3]. Another study developed an adaptive digital pre-distortion (ADPD) algorithm for LINC-based GaN PAs using a Field-Programmable Gate Array (FPGA), which achieved better linearity and higher efficiency [4].

In addition, researchers have investigated the impact of thermal distortion on LINC-based GaN PAs and proposed thermal models to better understand their behavior under high-temperature conditions [5]. A recent study proposed a new LINC architecture with a current-mode modulator to improve linearity and reduce complexity, which achieved high linearity and efficiency [6]. Furthermore, a machine learning-based LINC power amplifier linearization scheme was developed, which achieved better performance than conventional DPD methods [7].

Other recent studies have investigated the implementation of LINC-based GaN PAs in various wireless communication systems, including millimeter-wave (mmWave) and fifth generation (5G) communication systems. For example, a LINC-based mmWave PA was developed with improved linearity and efficiency [8]. Another study developed a LINC-based DPD technique for 5G communication systems, which achieved significant improvements in spectral regrowth and error vector magnitude [9].

FOREX Publication
Open Access | Rapid and quality publishing
International Journal of Electrical and Electronics Research (IJEER)
Research Article | Volume 12, Issue 4 | Pages 1418-1426 | e-ISSN: 2347-470X

Recent advancements in the field have highlighted different architectures for improving the efficiency of power amplifiers, such as Doherty, Out-phasing, and Envelope Tracking architectures, each presenting its own advantages and limitations in terms of performance and complexity [10]. A comparative study between an integrated Doherty power amplifier and an Out-phasing power amplifier for 5G communications demonstrated that while the Out-phasing amplifier offers better maximum power-added efficiency (PAE), the Doherty amplifier provides greater linearity and efficiency at specific output power levels [11]. Additionally, the use of an inverse Class-E architecture in Doherty amplifiers has allowed for increased efficiency and improved harmonic suppression levels [12]. Furthermore, the design and realization of high-efficiency, low-cost S-band GaN transmit/receive modules have demonstrated performance comparable to or exceeding state-of-the-art T/R modules available in the literature, highlighting the importance of thermal modelling and component management for reliable and reproducible mass production [13]. Finally, the integration of advanced technologies such as cognitive radio on satellite communication platforms, using GaN power amplifiers to dynamically adapt operating parameters, shows significant potential for flexible and autonomous communications in space environments [14, 15].

In summary, the LINC method is a powerful technique for improving the linearity of GaN PAs, and recent research has focused on developing new approaches for optimizing its performance. As wireless communication systems continue to evolve, the demand for high-power, high-efficiency PAs will continue to grow, making the LINC method an increasingly important tool in their design and optimization.

Power amplifiers (PAs) are among the most critical components in the design of wireless communication systems. Research on PAs that are both efficient and linear has started to focus more on the use of two-branch systems rather than traditional methods. The most popular dual-branch systems are the Doherty power amplifier [1–3], power amplifiers using envelope elimination and restoration (EER) techniques [4–6] and its variants, those designed by linear amplification with nonlinear components (LINC) and its derivative MILC. Other systems that fall into this category include the Chireix power amplifier system [7–9] and the phase-shift power amplifier [16, 17].

This paper is devoted to the application of the LINC linearization method [18], which is a derivative of the "out phasing" technique [19], to a GaN technology-based power amplifier. A CGH40010F high-electron-mobility transistor (HEMT) is selected to design the power amplifier. The (C/I) ratio [20] is chosen to measure the power amplifier's nonlinearity; for several reasons, the upper and lower C/I ratios may differ. In fact, the intermodulation distortion (IMD) [21–23] at $2\omega_1-\omega_2$ is different from that at $2\omega_2-\omega_1$.

2. MATERIALS AND METHODS

The CGH40010F transistor operating at 2.45 GHz is used to design the class AB power amplifier [24], and the operating point is set to VGS = -2.73 V and VDS = 28 V. This is a class AB biasing. The load-pull technique [25] requires a load tuner to vary the impedances seen by the device. It is then possible to plot constant output power contours (or constant power added efficiency contours) on the Smith chart. The optimal load corresponds to the smallest contours. A direct reading on the Smith chart then allows the value of the load impedance to be synthesized. The circuit of the load-pull analysis is shown in *figure 1*.

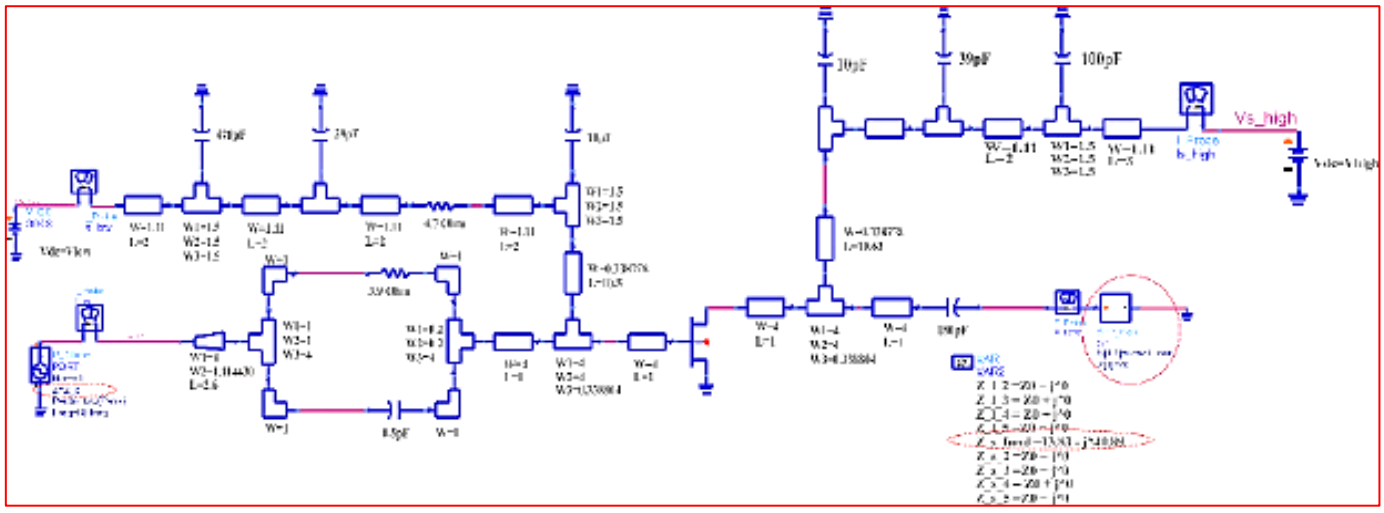

Figure 1. The circuit of the load-pull analysis

Load pull analysis is performed to obtain an idea of the optimal load and then to determine the input and output matching circuits of the power amplifier. The results of the load-pull simulations are represented in the form of contours in *figure 2.*

FOREX Publication
Open Access | Rapid and quality publishing
International Journal of Electrical and Electronics Research (IJEER)
Research Article | Volume 12, Issue 4 | Pages 1418-1426 | e-ISSN: 2347-470X

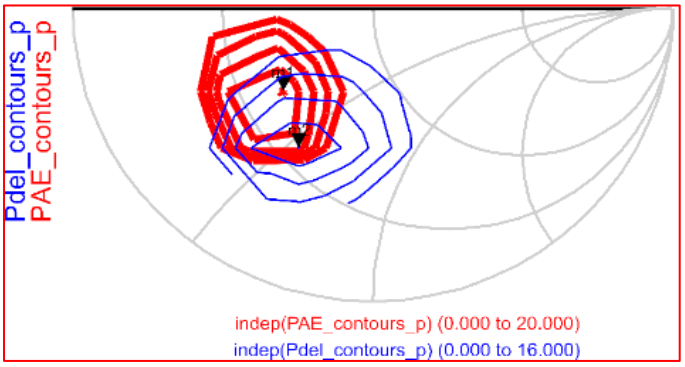

Figure 2. Load-pull contours of output power and power-added efficiency (PAE)

In *figure 3*, we can directly read the value of the optimal load which allows for maximum output power from the power amplifier, ZLopt = 13.5 - j21.40 Ω and Zs = 13.77 - j39.47 Ω. It corresponds to an output power of Pout = 41.5 dBm and a power-added efficiency (PAE) of 62.1%.

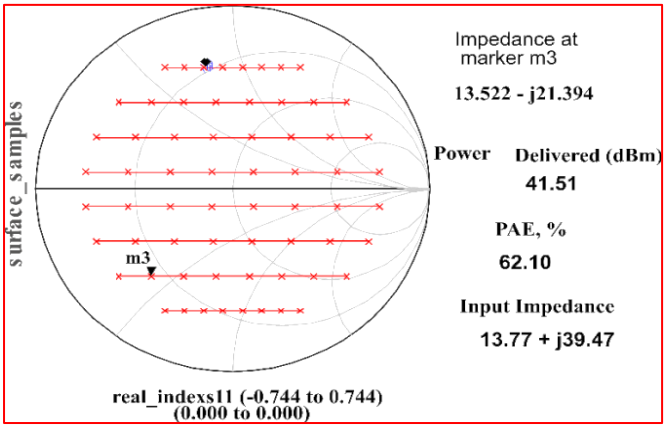

Figure 3. Simulated load impedance

2.1 Power Amplifier matching

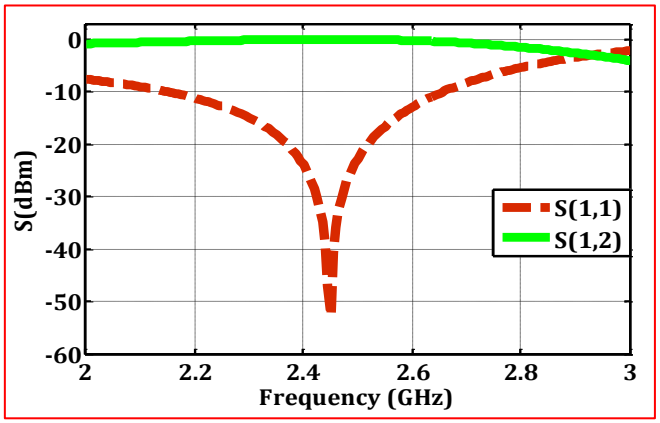

Figure 4. Verification of the Output matching circuit

Matching the input and output circuits is essential in the design of a power amplifier. The input and output matching networks are shown in *figure 6*. the *figures 4* and *figure 5* show the variations of the S (1,1) and S (2,2) parameters, we note that S (1,1) < 10 dB and S (2,2) < 10 dB The power amplifier is thus well matched at the input and output.

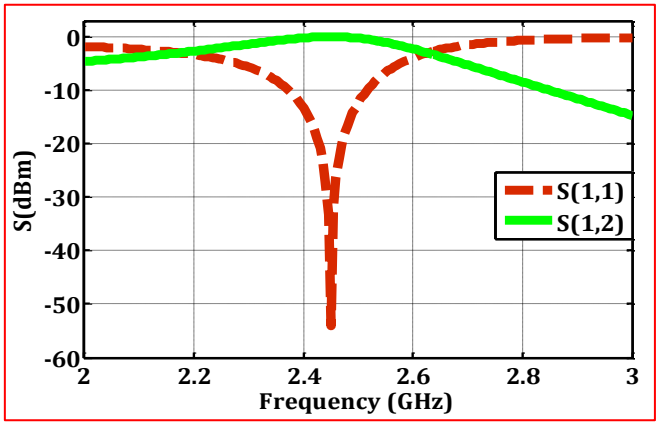

Figure 5. Verification of the input matching circuit

3. FINAL SCHEMATIC OF THE MAIN STAGE OF THE AMPLIFIER

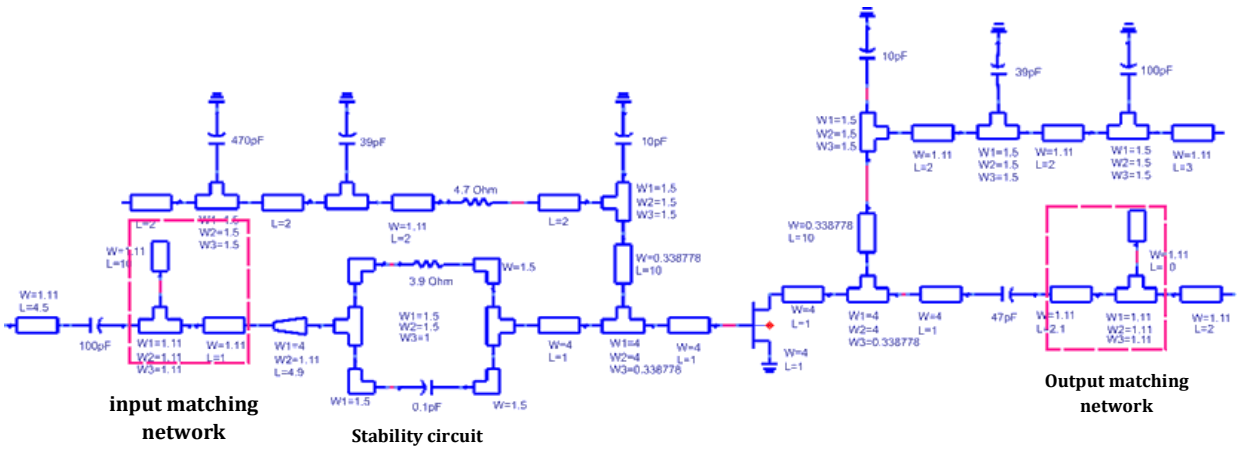

Figure 6. Power amplifier circuit

FOREX Publication
Open Access | Rapid and quality publishing
International Journal of Electrical and Electronics Research (IJEER)
Research Article | Volume 12, Issue 4 | Pages 1418-1426 | e-ISSN: 2347-470X

Figure 6 shows the complete circuit of the power amplifier biased at (28 V, -2.73 V). The circuit contains biasing and stability networks, matching networks, as well as other elements necessary for the design, such as quarter-wave transmission lines. *Figure 7* illustrates the generated layout of the power amplifier (20.2*36.5 mm2). Subsequently, different tests, such as single-tone and two-tone tests, will be applied to this power amplifier to determine its characteristics.

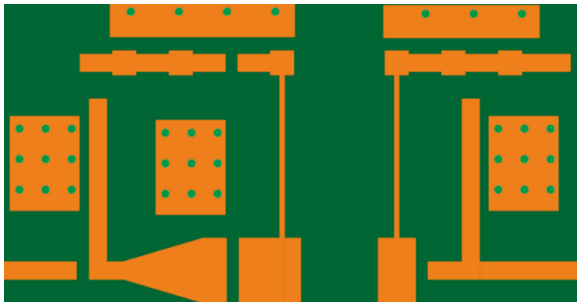

Figure 7. Layout of the power amplifier (20.2*36.5 mm2)

3.1 The single-tone signal test

The single-tone test determines certain important characteristics of the power amplifier, such as the P1dB point [26, 27], output power (Pout), power gain, and Power Added Efficiency (PAE) [28].

In my work [29], we can observe that the input power corresponding to the P1dB is approximately 28 dBm, leading to an output power of around 41.5 dBm, accompanied by a corresponding gain of roughly 13.5 dB, the Power Added Efficiency (PAE) reaches approximately 62%.

3.2 The two-tone signal test

The two-tone test is one of the best representations of signal excitations in telecommunications. It allows for the determination of different important characteristics of the power amplifier, such as the third-order intercept point (IP3), second-order intercept point (IP2), and the carrier-to-intermodulation ratio (C/I). The two input frequencies are set at (2.45 ± 0.005) GHz.

Figure 8 shows the third-order intercept point (IP3 or TOI). We can notice that the upper TOI is 46 dBm and the lower TOI is 62.5 dBm.

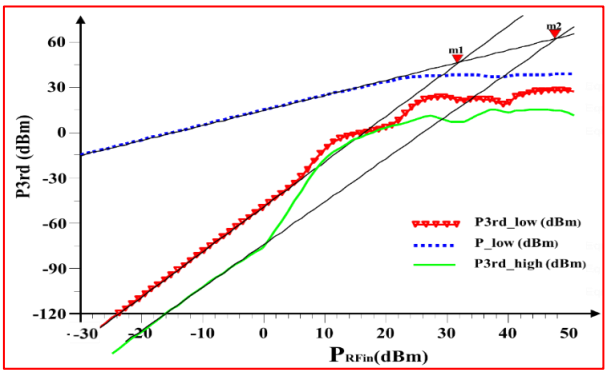

Figure 8. Simulated values for the TOI

The output spectrum of the power amplifier is shown in *figure 9* and *figure 10*. It can be seen that C/I_upper = 14 dBc and C/I_lower = 14.5 dBc, indicating that the power amplifier is nonlinear. To address this issue, the LINC method is applied.

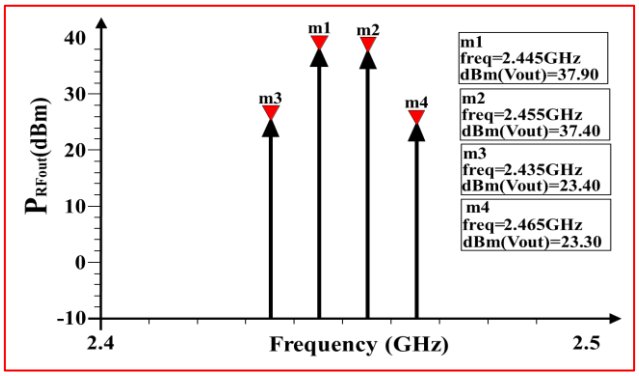

Figure 9. Output spectrum for the two-tone test of the power amplifier

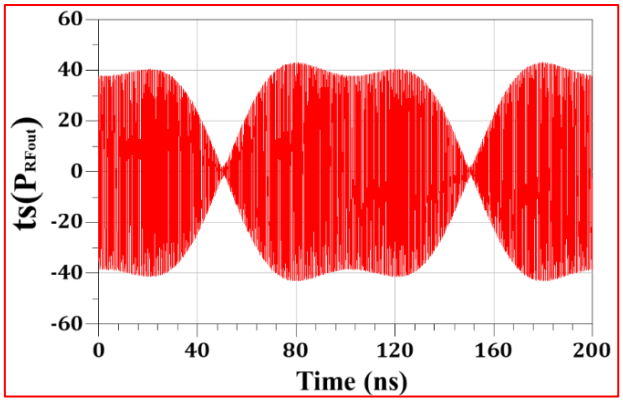

Figure 10. The temporal Output for the power amplifier

4. THEORY AND CALCULATION OF THE LINEARIZATION METHOD

The Linearization with no linear components separates input signal into two signals that are independently amplified by two identical nonlinear amplifiers, and then combined using a combiner, to obtain one output signal V_{out}, which is a linear amplification of the input signal. There are three main components in the LINC transmitter, which are the signal separator, the nonlinear amplifiers, and the signal combiner as shown in *figure 11*.

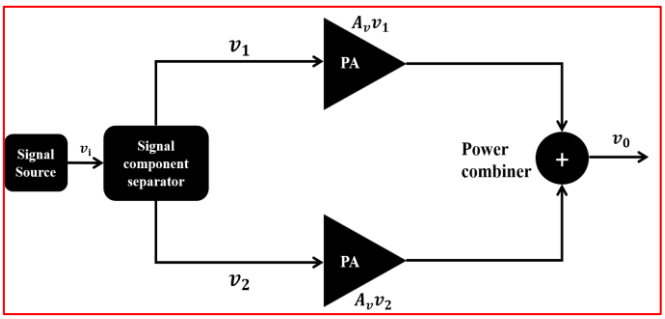

Figure 11. The LINC transmitter

FOREX Publication
Open Access | Rapid and quality publishing
International Journal of Electrical and Electronics Research (IJEER)
Research Article | Volume 12, Issue 4 | Pages 1418-1426 | e-ISSN: 2347-470X

The formula bellow describes the input signal:

$$S_i = S(t)\cos[\omega ct + \emptyset(t)] = \cos[\omega ct + \emptyset(t)]\cos[\arccos S(t)] \quad (1)$$

The expressions provided below illustrate the signals found in the outputs of the splitter. These signals can be understood as the combination of two signals from the previous expression.

$$S_1 = \frac{1}{2}\cos[\omega ct + \emptyset(t) + \arccos S(t)] \quad (2)$$

$$S_2 = \frac{1}{2}\cos[\omega ct + \emptyset(t) - \arccos S(t)] \quad (3)$$

The two signals S_1 and S_2 will be amplified by two power amplifiers with the same voltage gain Av. The final output signal will be given as follows:

$$S_0 = Av(S1 + S2)$$

$$S_0 = Av\{\frac{1}{2}\cos[\omega ct + \emptyset(t) + \arccos S(t)] + \cos[\omega c + \emptyset(t) - \arccos S(t)]\}$$

$$S_0 = AvS(t)\cos[\omega ct + \emptyset(t)] \quad (4)$$

The linearization with Nonlinear Components Method (LINC) method is used to linearize the power amplifier.

3.1 Results and discussion

The main and auxiliary power amplifiers were matched at the input and output, respectively. The input signal is split into two signals and combined using a coupler. The results of the simulation after linearization are shown in *figure 12*. *Figure 13* represents a comparison of the results before and after linearization. The basic diagram and the generated layout of the LINC system are reproduced in *figure 14* and *figure 15*, respectively.

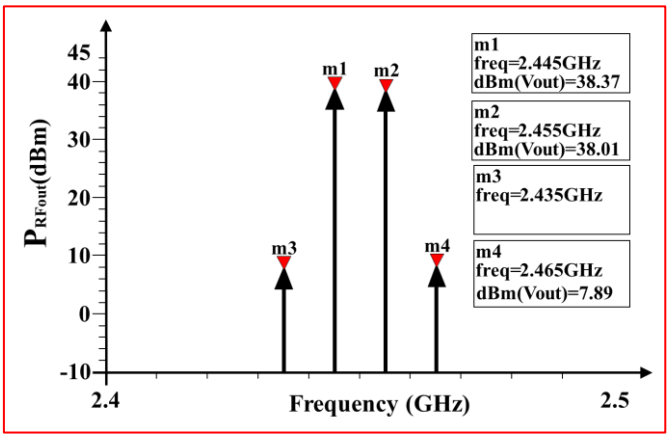

Figure 12. Simulated IMD3 after linearization

In *figure 12*, it can be observed that the C/I_upper = 30.9 dBc and the C/I_lower = 30 dBc, indicating good power amplifier linearization after applying the LINC method.

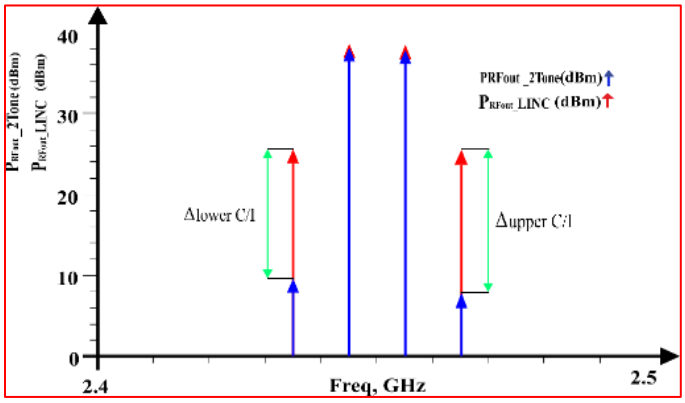

Figure 13. Comparison before and after linearization

In *figure 13*, we can see that the Δ_upper_C/I = 17 dBc and the Δ_lower_C/I = 15.5 dBc. The problem of non-linearity of the power amplifier is thus solved after the application of the LINC method.

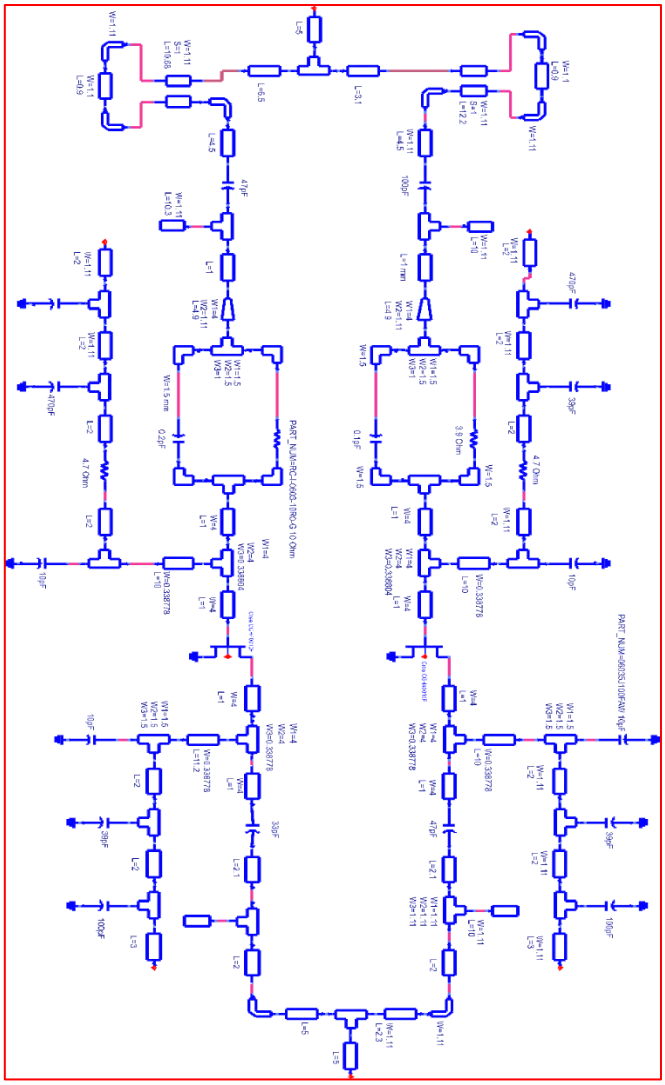

Figure 14. Basic diagram of the LINC system

FOREX Publication
Open Access | Rapid and quality publishing
International Journal of Electrical and Electronics Research (IJEER)
Research Article | Volume 12, Issue 4 | Pages 1418-1426 | e-ISSN: 2347-470X

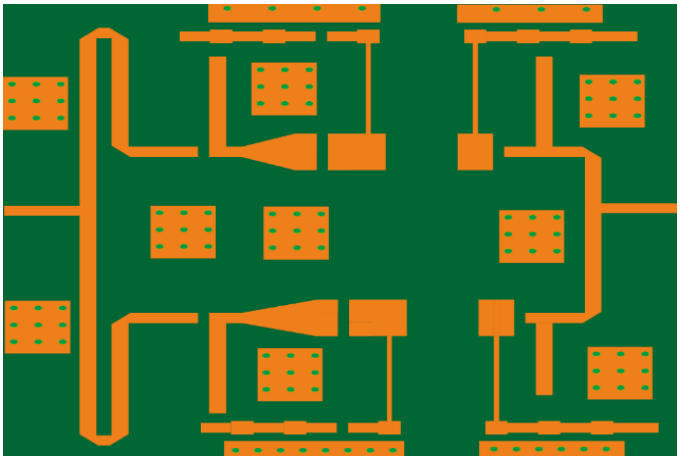

Figure 15. Layout of the LINC power amplifier

Table 1 summarizes the linearization results obtained after applying the LINC method. Δlower C/I and Δupper C/I are approximately 16 dBc and 17.3 dBc, respectively.

Table 1. C/I (carrier-to-interference) ratio performance

C/I (dBc)	C/I_upper (dBc)	C/I_lower (dBc)
Before LINC	13	12.5
After LINC	30.3	28.4
Linearization	Δ_upper_C/I = 17.3	Δ_lower_C/I = 16

5. ELECTROMAGNETIC SIMULATION (CO-SIMULATION HARMONIC BALANCE + MOMENTUM DU CIRCUIT)

The Momentum simulation [30], exclusively focuses on simulating the distributed segment of the circuit. Following this, an S-parameter model is created. Next, both linear and nonlinear localized components are integrated with the distributed segment, initiating the co-simulation process. *Figures 16* and *figure 17* provides a visual representation of the co-simulation of the power amplifier and the LINC method respectively. The outcomes of the simulation are presented in their respective figures, as seen in *figure 18*, *figure 19* and *figure 20*.

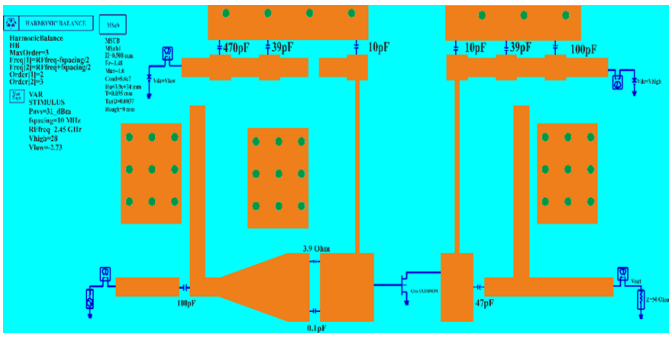

Figure 16. Power amplifier HB + Momentum co-simulation

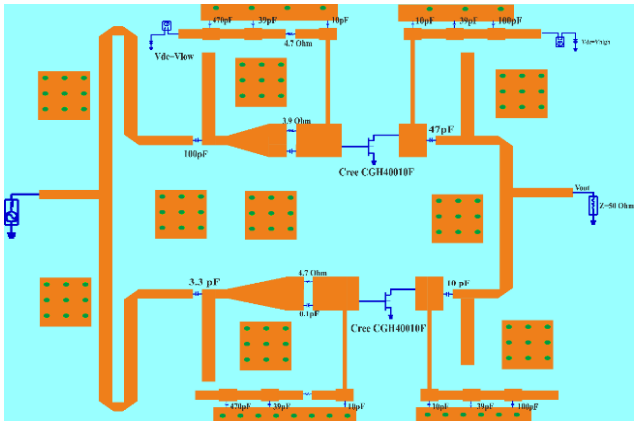

Figure 17. LINC HB + Momentum co-simulation

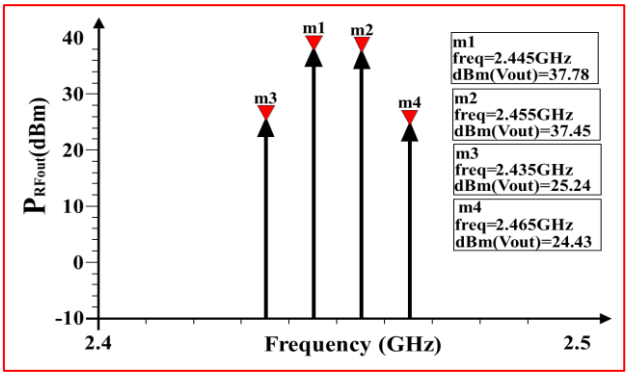

Figure 18. Power amplifier Output spectrum for HB + Momentum co-simulation

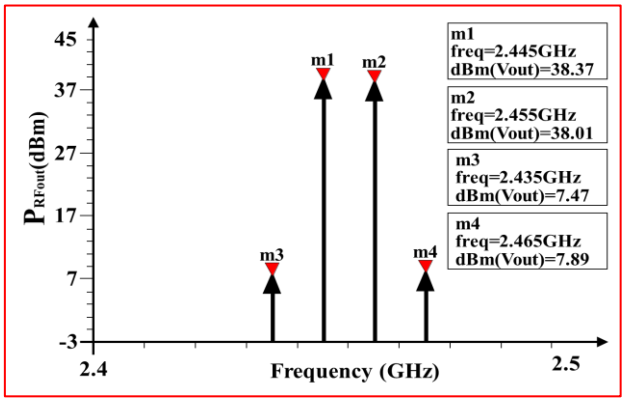

Figure 19. Output spectrum for LINC HB + Momentum co-simulation

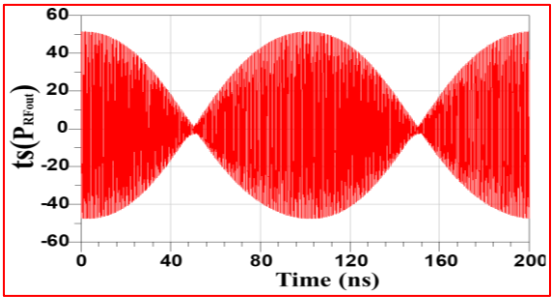

Figure 20. The temporal Output for LINC HB + Momentum co-simulation

FOREX Publication
Open Access | Rapid and quality publishing
International Journal of Electrical and Electronics Research (IJEER)
Research Article | Volume 12, Issue 4 | Pages 1418-1426 | e-ISSN: 2347-470X

In *figure 18*, we notice that the C/I_upper ratio is 13 dBc and the C/I_lower ratio is 12.6 dBc, whereas, in *figure19*, we notice that the C/I_upper ratio is 30.2 dBc and the C/I_lower ratio is 28.4 dBc, indicating that the non-linearity issue of the power amplifier has been resolved after the application of the LINC method. *Table 2* summarizes the linearization results obtained after the HB + Momentum co-simulation of the LINC method, which is very close to those obtained by schematic simulation.

Table 2. C/I ratio performance after HB + Momentum co-simulation

C/I (dBc)	C/I_upper (dBc)	C/I_lower (dBc)
Before LINC	12.6	13
After LINC	30.2	28.4
Linearization	Δ_upper_C/I = 17.6	Δ_lower_C/I = 15.4

6. DISCUSS PRACTICAL CHALLENGES

The LINC architecture is inherently more complex than conventional linearization methods. It requires precise synchronization between two amplifiers, which can introduce challenges in signal processing and circuit design. The need for accurate matching of the amplifiers' gains and phases is critical to ensure proper linear representation of the input signal.

The LINC technique typically involves additional components and circuitry compared to traditional linearization methods, leading to increased manufacturing costs. The need for high-quality nonlinear amplifiers, signal separators, and combiners can significantly elevate the overall expense of the amplifier design.

In practical applications, LINC can face issues such as thermal management and reliability. GaN amplifiers can generate significant heat, which may affect performance and longevity. The LINC method's reliance on precise component matching can also make the system sensitive to variations in temperature and component aging, potentially leading to degraded performance over time.

7. THE REALIZATION OF THE LINEARIZED AMPLIFIER IS DESCRIBED IN THIS SECTION

Figure 20 shows a photograph of the complete, assembled amplifier which measures 52.5 x 44.6 mm². The substrate used for this realization is the double-sided ROGERS RO4350B with a relative dielectric constant of εr = 3.48 and a thickness of h = 0.508 mm. *Table 3* provides a detailed BOM (Bill of Materials) of the equipment used for this work.

Table 3. Detailed bill of materials (BOM)

Reference	Fabricant	Code of fabrication	Description / Value	Paquet	Type
Q1, Q2	CREE	CGH40010F	10 W, GaN HEMT		
R1, R4	International Mfg Service	International Mfg Service RC-I Series	RC-I-0603-4R70-G 4.7 Ohm	0603	SMD
R2, R3	International Mfg Service	International Mfg Service RC-I Series	RC-I-0603-3R90-G 3.9 Ohm	0603	SMD
C1, C13	kemet	SMD Comm C0G, C0603C101F5	CAP CER 100pF	0603	SMD
C2, C5, C14, C17	kemet	SMD Comm C0G, C0603C390F5G	CAP CER 39pF	0603	SMD
C3, C4, C15, C16	kemet	SMD Comm C0G, C0603C100C5G	CAP CER 10pF	0603	SMD
C7	kemet	SMD Comm C0G, C0603C221F5G	CAP CER 220 pF	0603	SMD
C8	kemet	SMD Comm C0G, C0603C109C5G	CAP CER 1pF 0.25 pF	0603	SMD
C9	kemet	SMD Comm C0G, C0603C330F5G	CAP CER 33pF	0603	SMD
C10	kemet	SMD Comm C0G, C0603C470F5G	CAP CER 47 pF	0603	SMD
C11	kemet	SMD Comm C0G, C0603C159C5G	CAP CER 1.5pF 0.25 pF	0603	SMD
C12	kemet	SMD Comm C0G, C0603C229C5G	CAP CER 2.2pF 0.25 pF	0603	SMD
C6, C18	kemet	SMD Comm X7R, C0603C471J5R	CAP CER 470 pF	0603	SMD
P1, P2		CONN SMA STR PANEL JACK RECP			

FOREX Publication
Open Access | Rapid and quality publishing
International Journal of Electrical and Electronics Research (IJEER)
Research Article | Volume 12, Issue 4 | Pages 1418-1426 | e-ISSN: 2347-470X

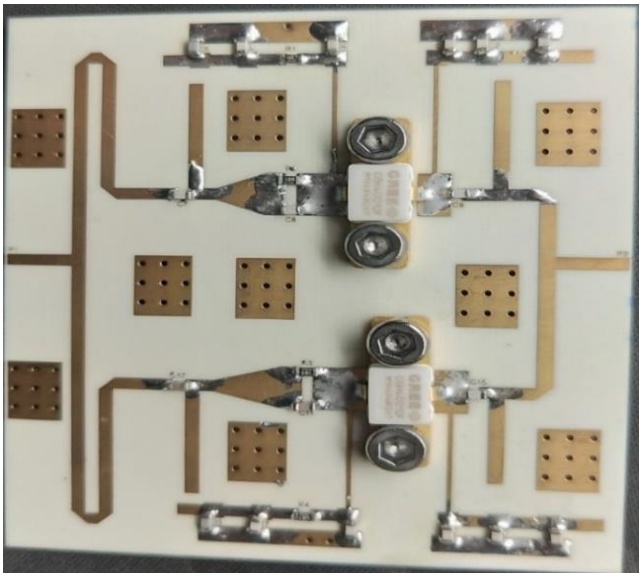

Figure 20. Photograph of the LINC power amplifier

8. COMPARATIVE ANALYSIS

Table 4 show the comparisons with other similar GaN amplifiers

Table 4. Comparison of different architectures of PA design

Ref	Architecture	Output Power	Efficiency
Elkhaldi et al. [1]	LINC	41.5 dBm	62.1%
Asbeck et al. [31]	Chirex outphasing	23 dBm	23%
Rostomyan et al. [32]	Doherty	22.4 dBm	40 %
Cappello et al. [33]	Supply modulation with digital predistortion	34 dBm	22.4–43.9%

9. CONCLUSION

This study focused on designing, optimizing, and linearizing a 2.45 GHz GaN-based RF power amplifier utilizing the CGH40010F transistor. Initially, a simple tone test characterized the amplifier, revealing an output power of approximately 41.5 dBm, a gain of 13.5 dB, and a PAE of 62%. However, during a two-tone test, noticeable non-linear behavior was observed, with elevated C/I ratios in both upper and lower sidebands, with Δ_sup = 18 dBc and Δ_inf C/I = 15.5 dBc. To enhance the amplifier's linearity, the LINC technique was employed. Simulations and co-simulations demonstrated significant improvements in linearity, resulting in Δupper C/I = 17.3 dBc and Δlower C/I = 16 dBc. Subsequently, the LINC linearization technique was successfully implemented on a printed circuit board, resulting in an improved, linearized amplifier. The results affirm the efficacy of the LINC method in enhancing the linearity of RF power amplifiers, a pivotal factor in ensuring the proper operation of wireless communication systems. Future work could explore several avenues to build upon these findings. One potential direction is to investigate the integration of digital pre-distortion (DPD) techniques alongside the LINC method to further enhance linearity and efficiency. Additionally, experimenting with advanced machine learning algorithms for real-time adaptation and optimization of the LINC parameters could provide significant improvements in dynamic wireless communication environments. Moreover, expanding this research to cover higher frequency bands, such as those used in millimeter-wave (mmWave) and 5G applications, could offer valuable insights into the scalability and versatility of the LINC technique. Finally, conducting extensive experimental validation in real-world scenarios will be essential to ensure the practical applicability and robustness of the proposed solutions.

REFERENCES

[1] Elkhaldi, S.; et al. LINC Method for MMIC Power Amplifier Linearization. Recent Adv. Electr. Electron. Eng. 2019, 12, 402-407.

[2] Hassan, N.U.; et al. Dense Small Satellite Networks for Modern Terrestrial Communication Systems: Benefits, Infrastructure, and Technologies. IEEE Wireless Commun. 2020, 27, 96-103.

[3] Elsayed, F.; Helaoui, M. Linearized Multi-Level Modulated Wireless Transmitters for SDR Applications Using Simple DLGA Algorithm. IEEE J. Emerg. Sel. Top. Circuits

[4] Letters, C. EERF6311 - Final Design Project, Sachin Kumar Asokan, August 2006.

[5] Perreault, D.J. A New Power Combining and Outphasing Modulation System for High-Efficiency Power Amplification. IEEE Trans. Circuits Syst. I Regul. Pap. 2011, 58, 1713-1726.

[6] Barton, T.W.; Perreault, D.J. Theory and Implementation of RF-Input Outphasing Power Amplification. IEEE Trans. Microw. Theory Tech. 2015, 63, 4273-4283.

[7] Baylis, C.; Moldovan, M.; Wang, L.; Martin, J. LINC Power Amplifiers for Reducing Out-of-Band Spectral Re-Growth: A Comparative Study. In Proceedings of the 2010 IEEE 11th Annual Wireless and Microwave Technology Conference (WAMICON 2010), 2010.

[8] De Falco, P.E.; et al. Load Modulation of Harmonically Tuned Amplifiers and Application to Outphasing Systems. IEEE Trans. Microw. Theory Tech. 2017, 65,

[9] Yahyavi, M. On the Design of High-Efficiency RF Doherty Power Amplifiers, 2016.

[10] Saurabh, K., Singh, S. Architectures for Efficiency Enhancement in Power Amplifiers. J. Inst. Eng. India Ser. B 105, 385–396, 2024.

[11] V. Díez-Acereda, S. L. Khemchandani, J. del Pino, et A. Diaz-Carballo. A Comparative Analysis of Doherty and Outphasing MMIC GaN Power Amplifiers for 5G Applications. Micromachines, vol. 14, no 6, 2023.

[12] A. Sheikhi, H. Hemesi, et A. Grebennikov, « Employing inverse Class-E power amplifier series output filter in parallel Doherty power amplifier. Microwave and Optical Technology Letters: Volume 65, Issue 2, Pages: 381-722, 2023.

[13] V. Kumar, Shreeshail, K. S. Beenamole and R. K. Gangwar. High Performance S-Band GaN T/R Module Using Hybrid Microwave Integrated Circuit. in IEEE Access, vol. 12, pp. 43089-43108, 2024.

[14] R. N. Simons, A. M. Gannon, J. A. Downey, M. T. Piasecki and B. L. Schoenholz, "Benefits of Ka-band GaN MMIC High Power Amplifiers with Wide Bandwidth and High Spectral/Power Added Efficiencies for Cognitive Radio Platforms," 2023 IEEE Cognitive Communications for Aerospace Applications Workshop (CCAAW), Cleveland, OH, USA, pp. 1-6, 2023.

FOREX Publication
Open Access | Rapid and quality publishing
International Journal of Electrical and Electronics Research (IJEER)
Research Article | Volume 12, Issue 4 | Pages 1418-1426 | e-ISSN: 2347-470X

[15] Zahid, M.N., Javeed, F. & Zhu, G. Design analysis of advanced power amplifiers for 5G wireless applications: a survey. Analog Integr Circ Sig Process 118, 199–217. 2024.

[16] Elkhaldi, S.; Touhami, N.A.; Aghoutane, M.; Elhamadi, T.E. LINC Method for MMIC Power Amplifier Linearization. Recent Adv. Electr. Electron. Eng. 2018, 12, 402-407.

[17] Singh, S.; Malik, J. Review of Efficiency Enhancement Techniques and Linearization Techniques for Power Amplifier. Int. J. Circuit Theory Appl. 2021, 49, 762-777.

[18] Elkhaldi, S.; Moubadir, M.; Touhami, N.A.; Aghoutane, M.; Elhamadi, T. Carrier to Intermodulation (C/I ratio) Calculations of a GaN 10W Class AB Power Amplifier. Int. J. Innov. Technol. Explor. Eng. 2020, 9, 887-890.

[19] Alim, M.A.; Tahsin, A.; Rezazadeh, A.A.; Gaquiere, C. Extraction of Nonlinear Taylor Series Coefficients for GaN HEMT over Multi-Bias Condition. Microelectronics J. 2020, 96, 104700.

[20] Yang, Q.K.; Liu, Y.A.; Yu, C.P.; Li, S.L.; Li, J.C. Design and Implementation of a High-Efficiency Concurrent Dual-Band Power Amplifier. J. China Univ. Posts Telecommun. 2014, 21, 94-99.

[21] Malik, W.A.; Sheta, A.A.; Elshafiey, I. Development of Efficient High-Power Amplifier with More Than an Octave Bandwidth. IEEE Access 2018, 6, 6602-6609.

[22] Zaveri, P. Analysis & Designing of RF Transistor as an Amplifier with Its Parametric Limitations. 2014, 5, 1524-1530.

[23] Pradeep, K.S.; et al. Design and Implementation of Class-F GaN HEMT Power Amplifier for S-Band Radar. In Proceedings of the 2017 International Conference on Electrical, Electronics, Communication, Computer, and Optimization Techniques (ICEECCOT), IEEE, 2017.

[24] Ji, Q.; et al. Design of Continuous Class-F Mode Power Amplifier with High Gain Flatness. J. Phys. Conf. Ser. 2022, 2221, 012001

[25] Petricli, I.; Riccardi, D.; Mazzanti, A. D-Band SiGe BiCMOS Power Amplifier with 16.8 dBm P_{1dB} and 17.1% PAE Enhanced by Current-Clamping in Multiple Common-Base Stages. IEEE Microw. Wirel. Compon. Lett. 2021, 31, 288-291.

[26] Malik, W.A.; Sheta, A.A.; Elshafiey, I. Development of Efficient High Power Amplifier with More Than an Octave Bandwidth. IEEE Access 2018, 6, 6602-6609.

[27] Chen, L.; et al. A Compact E-Band Power Amplifier with Gain-Boosting and Efficiency Enhancement. IEEE Trans. Microw. Theory Tech. 2020, 68.

[28] Hallberg, W.; et al. A Doherty Power Amplifier Design Method for Improved Efficiency and Linearity. IEEE Trans. Microw. Theory Tech. 2016, 64, 4491-4504.

[29] Elkhaldi, S.; El Bakkali, M.; Moubadir, M.; Aghoutane, M.; Touhami, N.A.; Elhamadi, T.E. Design and Electromagnetic Simulation of a 40 dBm Class-AB GaN Power Amplifier. In Proceedings of the 2020 International Symposium on Advanced Electrical and Communication Technologies (ISAECT), IEEE, 2020, pp. 1-5.

[30] Zhou, Han, et al. "A wideband and highly efficient circulator load modulated power amplifier architecture." IEEE Transactions on Circuits and Systems I: Regular Papers 70.8 (2023): 3117-3129.

[31] Asbeck PM, Rostomyan N, Özen M, Rabet B, Jayamon JA. Power Amplifiers for mm-Wave 5G applications: technology comparisons and CMOS-SOI demonstration circuits. IEEE Trans Microw Theory Tech. 2019;67(7):3099-3109.

[32] Rostomyan N, Ozen M, Asbeck P. 28 GHz Doherty power amplifier in CMOS SOI with 28% back-off PAE. IEEE Microw Wirel Components Lett. 2018;28(5):446-448.

[33] Cappello T, Pednekar P, Florian C, Cripps S, Popovic Z, Barton TW. Supply- and load-modulated balanced amplifier for efficient Broadband 5G base stations. IEEE Trans Microw Theory Tech. 2019;67(7):3122-3133